

Joint Approximate Diagonalization approach to Quasiparticle Self-Consistent GW calculations

Ivan Duchemin¹ and Xavier Blase²

¹*Univ. Grenoble Alpes, CEA, IRIG-MEM-L_Sim, 38054 Grenoble, France^{a)}*

²*Univ. Grenoble Alpes, CNRS, Institut Néel, F-38042 Grenoble, France*

(Dated: 5 December 2024)

We introduce an alternative route to quasiparticle self-consistent GW calculations (qs GW) on the basis of a Joint Approximate Diagonalization of the one-body GW Green's functions $G(\epsilon_n^{QP})$ taken at the input quasiparticle energies. Such an approach allows working with the full dynamical self-energy, without approximating the latter by a symmetrized static form as in the standard qs GW scheme. Calculations on the $GW100$ molecular test set lead nevertheless to a good agreement, at the 65 meV mean-absolute-error accuracy on the ionization potential, with respect to the conventional qs GW approach. We show further that constructing the density matrix from the full Green's function as in the fully self-consistent sc GW scheme, and not from the occupied quasiparticle one-body orbitals, allows obtaining a scheme intermediate between qs GW and sc GW approaches, closer to CCSD(T) reference values.

^{a)}Electronic mail: ivan.duchemin@cea.fr

I. INTRODUCTION

The Green's function many-body GW perturbation theory¹⁻⁴ has become a tool of choice in condensed-matter physics for the description of charged excitations, i.e. the electronic energy levels as obtained with photoemission experiments. Following pioneering application to the electron gas¹ or simple semiconductors, insulators and polymers,⁵⁻⁸ the GW formalism is now being used with much success as well in the study of molecular systems where it can be compared to other perturbative approaches such as coupled-cluster techniques.⁹⁻¹¹ The favorable scaling of the GW formalism, from quartic in its most common resolution-of-the-identity implementation,¹² to cubic and below, adopting space-time,¹³⁻¹⁹ moment-conserving²⁰ or stochastic^{21,22} techniques, contributes significantly to the success of this approach, together with the ability to deal with finite size or periodic, insulating or metallic, systems.

In its most common historical implementation, the needed time-ordered Green's function G and independent-electron susceptibility χ_0 , used to build the screened Coulomb potential W , are constructed from input one-body orbitals generated within mean-field Hartree-Fock (HF) or Kohn-Sham density functional theory (DFT). Such a relatively simple scheme is labeled the non-self-consistent, or single-shot, G_0W_0 formalism, an efficient approach that however provides results that depend on the input Kohn-Sham orbitals. The G_0W_0 results may prove not as reliable as needed if the input mean-field solution (charge-density, energy levels, orbitals shape, etc.) turns out to be very inaccurate.

A first strategy to improve the accuracy of G_0W_0 calculations consists in optimizing the input mean-field orbitals using, e.g., optimally tuned global or range-separated hybrids. The amount of exact exchange or the range-separation parameter can be tuned by satisfying e.g. the condition that the negative of the Kohn-Sham highest occupied orbital energy matches the ionization potential calculated within a more accurate Δ SCF calculation.²³ Such an approach is very efficient and popular in particular in the case of molecular systems.²⁴⁻²⁸

In the case of infinite periodic systems, the difficulties associated with Δ SCF calculations, and the cost of calculating the exact exchange contribution as compared to purely (semi)local functionals, lead to consider instead self-consistent schemes. Very early,⁶ a partially self-consistent scheme, with update of the quasiparticle energies only, was suggested, and studied extensively for solids²⁹⁻³¹ and molecular systems.^{27,28} Such a simple self-consistent scheme is often labeled $evGW$ and can be further simplified in a scissor-like approach.³²⁻³⁴

Full self-consistency beyond the *evGW* scheme was first introduced for a simple 1D model system,³⁵ the interacting homogeneous electron gas at varying density^{36,37} and simple metals or semiconductors.^{38–43} In such studies, the Green’s function is updated self-consistently together with the screened Coulomb potential treated as a functional of G through the dependence of the independent electron susceptibility on G (in short, $i\chi_0 = GG$). The self-consistent variable is thus the non-local energy-dependent $G(\mathbf{r}, \mathbf{r}'; E)$ time-ordered Green’s function, bypassing the need for one-body orbitals. This defines the fully self-consistent *scGW* approach that was used extensively to study molecular systems.^{44–56} Extensions to relativistic *scGW* schemes were further proposed for molecules containing heavy elements.⁵⁷

The fully self-consistent *scGW* was dramatically simplified by Faleev and coworkers who introduced a constrained self-consistency preserving the use of one-body wavefunctions.^{58,59} Such a quasiparticle self-consistent (*qsGW*) approach relies on an *ansatz* energy-independent symmetrized self-energy that upon diagonalization provides updated quasiparticle one-body wavefunctions and energies. This approach generalizes an early strategy where self-consistency was performed with the static Coulomb-Hole plus Screened Exchange (COHSEX) limit to the self-energy.⁶⁰ An equivalent Hamiltonian could be obtained by minimizing the total energy expressed as a functional of the one-body Green’s function, adopting the so-called Klein functional and minimizing over non-interacting Green’s functions.⁶¹ The *qsGW* scheme was extensively applied to solids^{41,56,58,59,62–66} and molecules,^{28,50,53,56,67–69} with extensions to two-components 2C-*qsGW* for molecules with heavy elements.⁷⁰ A different *qsGW* scheme was introduced by Kutepov *et al.*¹⁵ leading to a static self-energy through a linearization of its fully dynamical expression. For molecular systems, this second *qsGW* scheme was found to yield results close to the Shilfgaarde-Kotani-Faleev *qsGW* scheme.⁵⁶

Alternatively, Loos and coworkers introduced a similarity renormalization group approach to Green’s function methods,^{71,72} leading to a regularized definition of a static and hermitian self-energy, allowing to set up another formulation of a quasiparticle self-consistent *GW* scheme. Such an approach was further shown to cure difficulties associated with *GW* spectral functions dominated by several peaks.^{71–73}

A significant observation is that the *scGW* and *qsGW* ionization potential (IP) of small molecules was shown to differ by several tenths of an eV,^{50,53} with e.g. an average difference of 0.59 eV for the five primary nucleobases as part of the *GW100* test set.^{53,74–79} Overall, for the *GW100* test set, the IP mean-signed-error (MSE) was found to amount to -0.30/+0.15 eV for *scGW/qsGW* as compared

to CCSD(T) calculations.⁵³ In a recent study performed on a partially different set of 29 small molecules,⁷⁶ the *scGW* scheme was found slightly more accurate than the *qsGW* scheme, with MAE on IPs of 0.24 and 0.28-0.29 eV, respectively, as compared to CCSD(T) calculations.⁵⁶ In agreement with the *GW100* case, the *scGW*/*qsGW* schemes were found to underestimate/overestimate the IP values as compared to CCSD(T). The *scGW* IPs of a set of larger acceptor molecules was also found to be systematically underestimated as compared to CCSD(T) reference calculations with a mean absolute error (MAE) of 0.6 eV, while on the contrary the electronic affinity (AE) was overestimated with a similar 0.61 eV MAE.⁵² The origin of these differences between the two self-consistent approaches was tentatively analyzed in terms of screening, charge density differences and different treatment of the kinetic energy.⁵³

We present in this study an alternative quasiparticle self-consistent *GW* scheme that does not rely on a symmetrized static self-energy *ansatz* but introduces the idea of Joint Approximate Diagonalization⁸⁰ (JAD) of the $G(\epsilon_n^{QP})$ set of Green's functions, with $\{\epsilon_n^{QP}\}$ the quasiparticle energies given as input. Such an approach provides the optimal one-body molecular orbitals maximizing the diagonality of the Green's function taken at the quasiparticle energies. As a central issue, the present scheme allows working with the full dynamical self-energy without any simplification. Our *qsGW*_{JAD} scheme is benchmarked over the *GW100* molecular test set for which reference def2-TZVPP CCSD(T),⁷⁵ *qsGW* and *scGW* calculations⁵³ are available. Remarkably, even though relying *a priori* on a very distinct rationale, the present quasiparticle self-consistent approach yields ionization potentials in good agreement with the conventional *qsGW* quasiparticle self-consistent approach. Further, updating the density matrix through integrating the Green's function along the imaginary axis, rather than summing the contributions from the occupied one-body orbitals, in a simple scheme intermediate between *qsGW* and *scGW*, is shown to yield a better agreement with CCSD(T) data, reducing the mean-signed-error to about 60 meV for the *GW100* test set ionization potentials.

II. THEORY

In this Section, we outline the very basics of the *GW* formalism,^{2,4,81-84} and start by discussing the traditional diagonal approximation for the self-energy expressed in the Kohn-Sham molecular orbitals basis. We then present non-self-consistent and self-consistent schemes where the quasiparticle energies are extracted from the Green's function spectral function, rather than from

the quasiparticle equation, without the need to assume any restricted form (diagonal, static and symmetrized, etc.) for the self-energy.

A. The GW formalism

Belonging to the family of Green's function many-body perturbation theories, the GW formalism takes as a central variable the one-body time-ordered Green's function:

$$G(\mathbf{r}, \mathbf{r}'; \omega) = \sum_n \frac{g_n(\mathbf{r})g_n^*(\mathbf{r}')}{\omega - \varepsilon_n + i\eta \times \text{sgn}(\varepsilon_n - E_F)} \quad (1)$$

with η a positive infinitesimal and E_F the Fermi energy. Formally, the functions $\{g_n(\mathbf{r})\}$ are Lehman weights that measure how the ground-state Fermi sea with one added electron/hole in (\mathbf{r}) overlaps with the $(N+1)/(N-1)$ -electrons n -th excited state. Similarly, the energy poles $\{\varepsilon_n\}$ are the proper charging energies, as measured e.g. by photoemission, namely the difference of total energy $E_n(N+1) - E_0(N)$ for empty states, and $E_0(N) - E_n(N-1)$ for occupied levels. Even in a finite size basis set of dimensionality N_{basis} , the number of poles of $G(\omega)$ can be larger than N_{basis} . Anticipating on the GW approximation to the self-energy, it was shown that the number of poles formally scales as the size of the one-hole-two-electron (2e-h) or two-electron-one-hole (e-2h) spaces.^{71,85,86}

Following Hedin,¹ a set of self-consistent equations can be formally derived, relating the electronic susceptibility operator χ , the screened Coulomb potential W , the Green's function G , the exchange-correlation self-energy operator Σ , and the higher-order (3-body) vertex correction Γ . To lowest order in the screened Coulomb potential, neglecting vertex corrections, the energy-dependent exchange-correlation self-energy $\Sigma(\mathbf{r}, \mathbf{r}'; E)$ can be written under the form of the GW approximation :

$$\Sigma^{GW}(\mathbf{r}, \mathbf{r}'; E) = \frac{i}{2\pi} \int_{-\infty}^{+\infty} d\omega e^{i\eta\omega} G(\mathbf{r}, \mathbf{r}'; E + \omega) W(\mathbf{r}, \mathbf{r}'; \omega) \quad (2)$$

with W the dynamically screened Coulomb potential built within the (direct) random phase approximation (RPA) :

$$W(\mathbf{r}, \mathbf{r}'; \omega) = V(\mathbf{r}, \mathbf{r}') + \int d\mathbf{r}_1 d\mathbf{r}_2 V(\mathbf{r}, \mathbf{r}_1) \chi_0(\mathbf{r}_1, \mathbf{r}_2; \omega) W(\mathbf{r}_2, \mathbf{r}'; \omega) \quad (3)$$

with $\chi_0(\mathbf{r}_1, \mathbf{r}_2; \omega)$ the independent-electron susceptibility and V the bare Coulomb potential. The GW approximation with the RPA screened Coulomb potential only contains ring diagrams and

comparisons with other Green’s functions approaches and coupled-cluster techniques have been proposed.^{9,10,87,88}

In practice, the needed input Green’s function and independent-electron susceptibility required to build a first approximation to the GW self-energy are constructed with input Kohn-Sham eigenstates $\{\epsilon_n^{KS}, \phi_n^{KS}\}$, with e.g.:

$$\chi_0(\mathbf{r}, \mathbf{r}'; \omega) = \sum_{mn} \frac{(f_m - f_n) \phi_m^{KS}(\mathbf{r})^* \phi_n^{KS}(\mathbf{r}) \phi_m^{KS}(\mathbf{r}') \phi_n^{KS}(\mathbf{r}')^*}{\omega - (\epsilon_n^{KS} - \epsilon_m^{KS}) + i\eta \times \text{sgn}(\epsilon_n^{KS} - \epsilon_m^{KS})} \quad (4)$$

with $\{f_{m/n}\}$ level occupation numbers. Similarly, an input Green’s function can be obtained by replacing the Lehman weights and charging energies in equation 1 by the Kohn-Sham molecular orbitals and electronic energy levels. This construction leads to a starting G_0W_0 “single-shot” self-energy that may strongly depend on the choice of the starting functional used to generate the input Kohn-Sham eigenstates. This dependence may be cured by performing self-consistent GW calculations as discussed below.

B. The diagonal self-energy approximation

Stemming from historical calculations in simple systems such as bulk silicon,^{6,7} it is commonly accepted that, in general, the Hamiltonian built with the GW self-energy is dominantly diagonal in the input Kohn-Sham basis. As such, the most common GW calculations adopt a diagonal approximation where the contribution from the spurious DFT exchange-correlation potential is replaced by the expectation value of the GW self-energy on the corresponding input Kohn-Sham eigenstate:

$$\epsilon_n^{GW} = \epsilon_n^{KS} + \langle \phi_n | \Sigma_{XC}^{GW}(\epsilon_n^{GW}) - V_{XC}^{DFT} | \phi_n \rangle \quad (5)$$

No off-diagonal self-energy matrix elements in the Kohn-Sham basis, namely $\langle \phi_n | \Sigma_{XC}^{GW}(\omega) | \phi_m \rangle$ ($n \neq m$) matrix elements, is ever calculated as in the quasiparticle self-consistent qsGW approach. Inspection of Eq. 5 shows that the quasiparticle energies directly depend on the quality of the diagonal approximation and on the shape of the input Kohn-Sham molecular orbitals.

Partial self-consistency in such a diagonal approximation can be performed by reinjecting the calculated quasiparticle energies in the construction of G and W , a popular scheme labeled evGW.^{28,31,89} The evGW scheme was shown to reduce significantly the dependence on the starting input Kohn-Sham molecular orbitals, even though for some systems such a dependence remains strong. We will provide an example here below.

C. Quasiparticle energies as the poles of the GW Green's function

An alternative approach to finding the quasiparticle energies consists in considering directly the poles of the one-body Green's functions. Taking on general grounds the spectral representation of G as given by Eq. 1, the expectation value of G on a specific input molecular orbital (ϕ_n) reads:

$$\langle \phi_n | G(\mathbf{r}, \mathbf{r}'; \omega) | \phi_n \rangle = \sum_m \frac{|\langle \phi_n | g_m \rangle|^2}{\omega - \varepsilon_m + i\eta \times \text{sgn}(\varepsilon_m - E_F)} \quad (6)$$

Clearly, the poles of $\langle \phi_n | G | \phi_n \rangle$ are independent of the chosen one-body wavefunctions representation $\{\phi_n\}$. Further, concerning specifically the GW Green's function:

$$G^{-1}(\omega) = G_{KS}^{-1}(\omega) + \Sigma_{XC}^{GW}(\omega) - V_{XC}^{DFT} \quad (7)$$

with G_{KS} the input Kohn-Sham Green's function, the search for the quasiparticle energies as the poles of G does not require assuming the diagonality of the self-energy in the input $\{\phi_n\}$ basis. Namely, the $\langle \phi_m | \Sigma_{XC}^{GW}(\omega) | \phi_n \rangle$ matrix is entirely considered and constructed with the fully dynamical self-energy as defined in eq. 2.

The quasiparticle energies can then be calculated by extracting the dominant pole(s) in the spectral representation of the diagonal matrix elements of the GW Green's function in the available one-body molecular orbitals (MOs), typically the input Kohn-Sham MOs or the quasiparticle MOs of the previous iteration in a qs GW scheme:

$$A_n^{GW}(\omega) = \frac{1}{\pi} |\mathcal{I}m(\langle \phi_n | G(\omega) | \phi_n \rangle)| \quad (8)$$

On formal grounds, this approach relies on the "quasiparticle" assumption, namely that $A_n^{GW}(\omega)$ will be dominated by a peak capturing most spectral weight, or a "forest" of peaks that can be well described by a Lorentzian envelop providing the ε_n^{QP} quasiparticle energy, the Z_n^{QP} spectral weight, and the associated Γ_n^{QP} lifetime:

$$A_n^{fit}(\omega) = \frac{1}{\pi} \left| \mathcal{I}m \left(\frac{Z_n^{QP}}{\omega - (\varepsilon_n^{QP} + i\Gamma_n^{QP})} \right) \right|$$

In particular, the only constraint on the ϕ_n one-body orbital is that it should overlap significantly with the Lehman weight(s) $\{g_m\}$ associated with the n-th quasiparticle energy. As stated above however, the quasiparticle energy does not depend on the choice of ϕ_n . Details about calculating and fitting the spectral function $A_n^{GW}(\omega)$ is described in Ref. 90 and in the Technical subsection below.

To illustrate the impact of releasing the diagonal approximation on the self-energy, and extracting the quasiparticle energies directly from the spectral function, we study the quasiparticle energies associated with the low lying unoccupied energy levels of carbon monoxide (CO). We keep here the input Kohn-Sham orbitals frozen, but perform a partial self-consistency on the quasiparticle energies, namely an *evGW* scheme. This allows studying specifically the impact of the choice of a given set of input wavefunctions. The results are reported in Fig. 1. The input Kohn-Sham orbitals are generated with the PBEh(α) global hybrids,⁹¹ with α ranging from zero (the PBE functional⁹²) to one (a hundred percent of exact exchange). Calculations are performed with the augmented aug-cc-pVTZ basis set^{93,94} to deal with diffuse states with positive energy.

The standard *evGW* results, using eq. 5, are represented by full black lines (*evGW* diag- Σ ; Fig. 1). Clearly, this standard scheme leads to a dramatic sensitivity of some of the lowest CO unoccupied energy levels with the amount of exact exchange in the starting Kohn-Sham functional, despite the self-consistency on the quasiparticle energies. In particular, the Kohn-Sham LUMO orbital becomes the LUMO+1 for a wide range of exact exchange percentage at the *evGW* diag- Σ

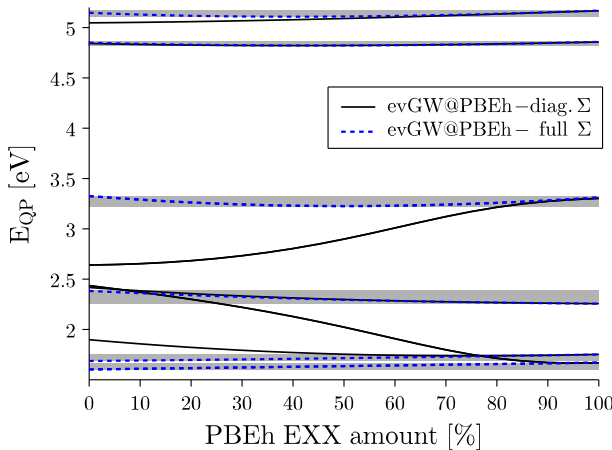


FIG. 1. Empty states energy levels for the CO molecule as obtained from *evGW* calculations with partial self-consistency on the eigenvalues. The energies are plotted as a function of the amount of exact exchange in the starting Kohn-Sham PBEh functional used to generate the input Kohn-Sham eigenstates. The traditional diagonal approximation on the self-energy operator (full black lines, *evGW*-diag. Σ) leads to a strong residual dependence on the starting functional for Rydberg states, while extracting the quasiparticle energies from the spectral function $A_n(\omega)$ (dashed blue lines; *evGW*-full Σ) dramatically stabilizes the *evGW* results. Calculations performed at the aug-cc-pVTZ level. Grey areas indicate the small variations of the *evGW* energy levels extracted from $A_n^{GW}(\omega)$. We adopt here the CC3/aug-cc-pVTZ geometry of Ref. 95.

level, only to fall back to the LUMO level when starting with a PBEh hybrid functional with more than $\sim 75\%$ of exact exchange. This is the signature that the associated Kohn-Sham wavefunctions strongly depend on the DFT XC functional. Such a sensitivity was shown⁹⁶ to originate from the diffuse nature of the unoccupied CO molecular orbitals that experience the significant change in the XC potential vacuum tail as a function of the amount of exact exchange.

We now calculate the full self-energy matrix $\Sigma_{XC}^{GW}(\omega)$ in the Kohn-Sham basis to build the *GW* Green’s function (eq. 7), capturing the quasiparticle energies ε_n^{QP} from the dominant peak in the related $A_n^{GW}(\omega)$. The results are represented by the dashed blue lines in Fig. 1 (ev*GW* full- Σ). Clearly, the obtained quasiparticle energies are much less sensitive to the choice of the input exchange-correlation (XC) functional and related one-body molecular orbitals (MOs). This illustrates that even without self-consistency on the one-body MOs, extracting the quasiparticle energies from the pole(s) of the diagonal matrix elements of G , but considering the full self-energy matrix in the input Kohn-Sham basis when building G , allows reducing dramatically the dependence of the quasiparticle energies on the input Kohn-Sham set of wavefunctions.

We note that the standard ev*GW* calculations, with the Σ -diagonal assumption, and the approach bypassing the diagonality assumption, provide very similar results for input Kohn-Sham XC functionals containing above 80% of exact exchange. Such a value is close to the 75% found in an IP-tuning strategy for CO.⁹⁶ Benchmark calculations on molecular systems^{27,97} supported the conclusion that standard *GW* calculations, with frozen input Kohn-Sham wavefunctions generated with an optimally-tuned Kohn-Sham functional, would lead to accurate *GW* calculations and, subsequently, related Bethe-Salpeter optical spectra.^{97,98} This is an indication that the approach relying on the $\langle \phi_n | G(\omega) | \phi_n \rangle$ spectral function, without assuming the diagonality of Σ operator in the KS basis, yields results that are not only much less dependent on the input Kohn-Sham molecular orbitals, but also close to the best non-self-consistent calculations relying on optimally tuned initial Kohn-Sham functionals.

D. Quasiparticle self-consistent *GW* approach with a Joint Approximate Diagonalization scheme

While working with the spectral function, bypassing the diagonal self-energy approximation, can reduce the impact of the input ϕ_n molecular orbitals (MO) on the quasiparticle energies, it is well documented that in many situations, self-consistency on the MOs becomes required. This is e.g. the

case of systems involving very localized d or f orbitals. Inaccurate KS MOs, of the kind obtained with purely local functionals, may lead to an erroneous density-matrix, spoiling the resulting Hartree and exchange potentials, and further to inaccurate response functions (susceptibility, screened Coulomb potential). In addition, subsequent post-processing of GW results, such as calculating the optical spectrum within the Bethe-Salpeter equation formalism, can be very sensitive to the shape of the MOs.^{98,99}

We then now proceed to a full quasiparticle self-consistent scheme (qsGW) that avoids relying on the diagonalization of an Hamiltonian based on an optimal *ansatz* static and symmetrized self-energy operator:

$$\Sigma_{nm}^{\text{qsGW}} \simeq \frac{1}{2} \langle \phi_n | \Sigma(\varepsilon_n) + \Sigma(\varepsilon_m) | \phi_m \rangle \quad (9)$$

as introduced by Faleev and coworkers.^{58,59} Following a common approach in signal processing, we adopt a *Joint Approximate Diagonalization (JAD)*⁸⁰ of the set of Green's function matrices taken at the quasiparticle energies. Namely, we look for a unitary rotation U within the input Kohn-Sham MOs that minimizes the off-diagonal matrix elements of the $\{G_n = G(\varepsilon_n^{QP})\}$ set of matrices. This joint minimization scheme can be formulated as:

$$\underset{U}{\operatorname{argmin}} \mathcal{F}(U, G_n) \quad (10)$$

with:

$$\mathcal{F}(U, G_n) = \sum_n^{N_{\text{orbs}}} \|\text{off-diag}(U^\dagger G(\varepsilon_n^{QP}) U)\| \quad (11)$$

where $\{U, G_n\}$ are expressed in the Kohn-Sham MO basis. The upper limit N_{orbs} indicates the number of Kohn-Sham orbitals that are allowed to mix, typically all occupied states and a large number of unoccupied states. As stated above, working with the GW Green's function allows preserving the fully dynamical GW self-energy as defined in eq. 2 without any approximation.

Qualitatively, we thus look for the optimal one-body wavefunction basis that maximizes the diagonality of the one-body Green's functions taken at the quasiparticle energies. While the standard qsGW scheme relies on the definition of a static symmetrized self-energy, here the approximation lies in that there is in general no rotated $\{U\phi_n^{KS}\}$ basis that can strictly diagonalize all $G(\varepsilon_n^{QP})$ matrices at the same time. The two approximations are thus *a priori* of different nature, even though both aiming at constructing "optimal" one-body quasiparticle $\{\varepsilon_n^{QP}, \phi_n^{QP}\}$ eigenstates.

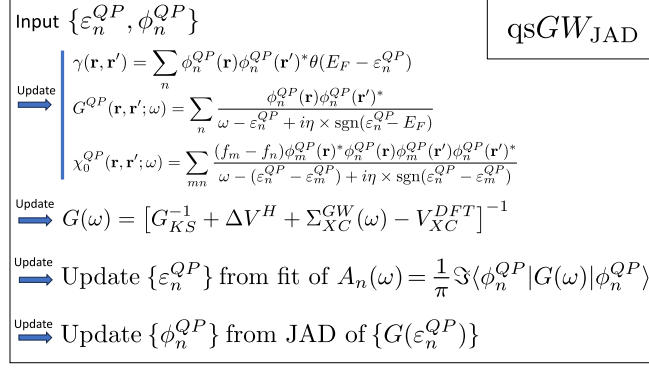


FIG. 2. Schematic representation of the qsGW_{JAD} self-consistent scheme.

The self-consistency proceeds by using these one-body eigenstates to update the density matrix:

$$\gamma(\mathbf{r}, \mathbf{r}') = \sum_n \phi_n^{QP}(\mathbf{r})\phi_n^{QP}(\mathbf{r}')^* \theta(E_F - \varepsilon_n^{QP}) \quad (12)$$

and associated charge-density, together with an updated Green's function to start the new iteration:

$$G^{QP}(\mathbf{r}, \mathbf{r}'; \omega) = \sum_n \frac{\phi_n^{QP}(\mathbf{r})\phi_n^{QP}(\mathbf{r}')^*}{\omega - \varepsilon_n^{QP} + i\eta \times \text{sgn}(\varepsilon_n - E_F)} \quad (13)$$

Likewise, an updated susceptibility is built replacing the KS eigenstates in eq. 4 by the quasiparticle eigenstates. This allows building an updated Hartree potential and Σ_{XC}^{GW} self-energy.

In the traditional qsGW scheme, Σ_{XC}^{GW} would be reduced to the static symmetrized ansatz as given by eq. 9 for direct diagonalization. In the present case, the full dynamical Σ_{XC}^{GW} is used to build an updated GW Green's function beyond the quasiparticle approximation:

$$G^{-1}(\omega) = G_{KS}^{-1}(\omega) + \Delta V_H + \Sigma_{XC}^{GW}(\omega) - V_{XC}^{DFT} \quad (14)$$

where ΔV_H is the variation of the Hartree potential with respect to the input KS one. After extracting the new quasiparticle energies ε_n^{QP} from the dominant pole(s) of the updated $G(\omega)$ and associated $A_n(\omega)$, the JAD of these new $G(\varepsilon_n^{QP})$ allows updating the quasiparticle one-body molecular orbitals to feed the next iteration. This scheme will be labeled here below the qsGW_{JAD} scheme (see schematic flow in Fig. 2). We emphasize that G^{QP} is really written in the quasiparticle form, with a spectral function consisting of N_{basis} δ -functions with weight $Z=1$ at the available input quasiparticle energies, with N_{basis} the size of the Kohn-Sham basis. G^{QP} only serves to build the updated self-energy Σ_{XC}^{GW} . On the contrary, G not only contains the quasiparticle peaks, with an associated $Z \leq 1$ spectral weight, but also the incoherent background.

Since the JAD scheme uses the self-energy as it stands, it can be straightforwardly merged with any form of dynamical self-energy extending beyond the GW approximation, including renormalized singles,^{100–102} second-order screened exchange,¹⁰³ and various forms of vertex corrections^{56,70,104–116} to the GW self-energy. Likewise, the present approach can be merged with other forms of self-energy, such as the GT approximation based on ladder diagrams, that has also been appraised for the calculation of the quasiparticle properties of molecular systems.^{117,118}

E. Modified qsGW with a density-matrix beyond the quasiparticle approximation

A simple alternative approach to the present $qsGW_{JAD}$ stems from the possibility to calculate the density-matrix $\gamma(\mathbf{r}, \mathbf{r}')$ by integrating along the imaginary axis the time-ordered Green’s function (eq. 14) :

$$\gamma(\mathbf{r}, \mathbf{r}') = \frac{1}{2} \left(\delta(\mathbf{r}, \mathbf{r}') + \frac{1}{\pi} \int_{-\infty}^{+\infty} d\omega G(\mathbf{r}, \mathbf{r}'; i\omega) \right) \quad (15)$$

and not from the rotated occupied $\{\phi_n^{QP} = U\phi_n^{KS}\}$ eigenstates. As such, the density-matrix in eq. 15 captures the contributions from the quasiparticle peaks and the incoherent background, as in a full $scGW$ self-consistent scheme. This leads to an internal loop where starting from the Hartree and exchange operators built with the density matrix of eq. 12, the Hartree and exchange contributions to G in eq. 14 are updated through eq. 15 keeping the correlation self-energy frozen. This does not cost significant time. Such an approach will be labeled the γsGW_{JAD} scheme, where the γs subscript indicates that the density-matrix is calculated as in the full self-consistent scheme. It remains that the GW self-energy is constructed with G^{QP} and the non-interacting susceptibility χ_0 built from one-body molecular orbitals. This approach adopts thus features from both the $qsGW$ and the fully-self-consistent $scGW$ schemes.

F. Technical details

Our calculations are performed with the `BEDEFT` (beyond-DFT) package^{19,90} implementing the GW and Bethe-Salpeter equation (BSE) formalisms with Gaussian basis sets and Coulomb-fitting (RI-V) resolution-of-the-identity techniques.^{12,119–121} We exploit in particular a recently improved analytic continuation (AC) scheme combined with the contour-deformation approach that allows calculating accurately the GW self-energy, even for levels located far away from the gap.⁹⁰ The independent electron susceptibility $\chi_0(z)$ and related RPA screened Coulomb potential $W(z)$ are

calculated for an optimized grid of N_ω frequencies ($z = i\omega$) along the imaginary frequency axis ($N_\omega = 14$), completed by a coarse grid of complex frequencies ($z = \omega + i\eta$) above the real-axis. This set of calculations allows setting an accurate analytic continued-fraction expression for the screened Coulomb potential, and consequently an analytic form for the self-energy and associated Green’s function. The stability of the quasiparticle energies with respect to the sampling grid, from core to unoccupied levels, was extensively studied in Ref. 90. Such an improved AC scheme was recently exploited by several groups in the study of core levels.^{90,122,123} Besides all occupied states, off-diagonal self-energy matrix elements are constructed with unoccupied states within an energy window of 200 eV above the gap. The JAD minimization process with respect to the unitary U operator matrix elements does not represent by itself a significant computational effort.

To allow comparison with previous qsGW and scGW studies of the highest-occupied molecular orbital (HOMO) energies for the so-called GW100 molecular test set,⁵³ with associated reference CCSD(T) data,⁷⁵ we adopt the def2-TZVPP basis set¹²⁴ and the corresponding optimized auxiliary basis set.¹²⁵ Input Kohn-Sham eigenstates are generated by the Orca package.¹²⁶ We adopt the PBE0 functional^{91,127} as the mean-field Kohn-Sham starting point. Following the qsGW and scGW reference calculations from Ref. 53, we exclude molecules containing fifthrow atoms for which all-electron def2-TZVPP basis sets are not available, reducing the GW100 test set to 93 molecules [see Table S1 in the Supplementary Material (SM)].

III. RESULTS

We start by providing in Fig. 3 (blue) a bar plot of the difference ($\epsilon_{HOMO}^{qsGW} - \epsilon_{HOMO}^{qsGW_{JAD}}$) for the set of 93 molecules extracted from the GW100 test set. The qsGW_{JAD} data are available in the Table S1 of the Supplementary Material (SM) while the ϵ_{HOMO}^{qsGW} are taken from Ref. 53. The present qsGW_{JAD} scheme yields as expected results slightly different from the original qsGW scheme. However, the associated mean-absolute-error (MAE) and mean-signed-error (MSE) are small, amounting to 65 meV and 3 meV, respectively. These deviations change to 56 meV and 13 meV if one removes the C_8H_8 outlier¹²⁸ for which the qsGW HOMO energy seems really off in the calculations of Ref. 53. For sake of comparison, we also plot the difference ($\epsilon_{HOMO}^{scGW} - \epsilon_{HOMO}^{qsGW_{JAD}}$) (red) on the basis of the scGW data from Ref. 53. Such a comparison shows that the two qsGW schemes are very close to each other as compared to the differences between the qsGW and scGW data. The MAE and MSE between qsGW_{JAD} and scGW are indeed much larger, amounting both to 0.45 eV. Such an

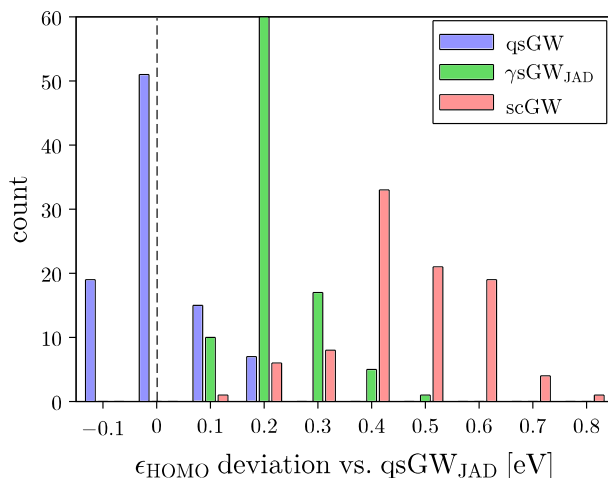


FIG. 3. Bar plot of the ϵ_{HOMO}^{qsGW} (blue), $\epsilon_{HOMO}^{\gamma^sGW_{JAD}}$ (green), and ϵ_{HOMO}^{scGW} (red) energies, taking as a reference the present $\epsilon_{HOMO}^{qsGW_{JAD}}$ values. The qsGW and scGW data are from Ref. 53, considering the full set of 93 molecules reported, except the C_8H_8 cyclooctatetraene molecule which really stands as an outlier taking the qsGW value of Ref. 53 (see Note 128). The $qsGW_{JAD}$ and γ^sGW_{JAD} data are available in the Table S1 of the SM.

agreement between qsGW and $qsGW_{JAD}$ data is rather remarkable given the very different nature of the approximations on which the two schemes are hinging.

We now compare in Fig. 4(a) the present $qsGW_{JAD}$ data to the CCSD(T) reference. The $qsGW_{JAD}$ scheme yields too deep HOMO levels, that is too large ionization potentials (IP), with MSE/MAE of -0.15 eV/0.21 eV, respectively. As expected, this is nearly identical to the MSE/MAE of -0.15 eV/0.22 eV characterizing the difference between qsGW and CCSD(T).¹²⁹ In particular, the error associated with the outliers (see corresponding names in Fig. 4), are close to what was found for the standard qsGW scheme (see values in Table S1 in the SM), except for the C_8H_8 outlier as discussed above.

We further examine in Fig. 4(b) the present γ^sGW_{JAD} data as compared to the CCSD(T) reference. As explained above, the update of the Hartree and exchange potentials are here performed by calculating the density matrix through an integral along the imaginary axis of the full Green's function $G = [G_{KS}^{-1} + \Delta V_H + \Sigma_{XC}^{GW} - V_{XC}^{DFT}]^{-1}$ (eqn. 14), and not as a sum over the occupied $\{\phi_n^{QP} = U\phi_n^{KS}\}$ rotated one-body wavefunctions. The associated results are found to be in better agreement with the CCSD(T) data. The corresponding MAE and MSE reduce to 156 meV and 62 meV, respectively. While qsGW and scGW show a deviation with respect to the CCSD(T) HOMO energy by -0.15 eV and 0.30 eV¹³⁰ (MSE values) respectively, this intermediate scheme yields data in between the two self-consistent GW approaches, closer to CCSD(T) reference. This is

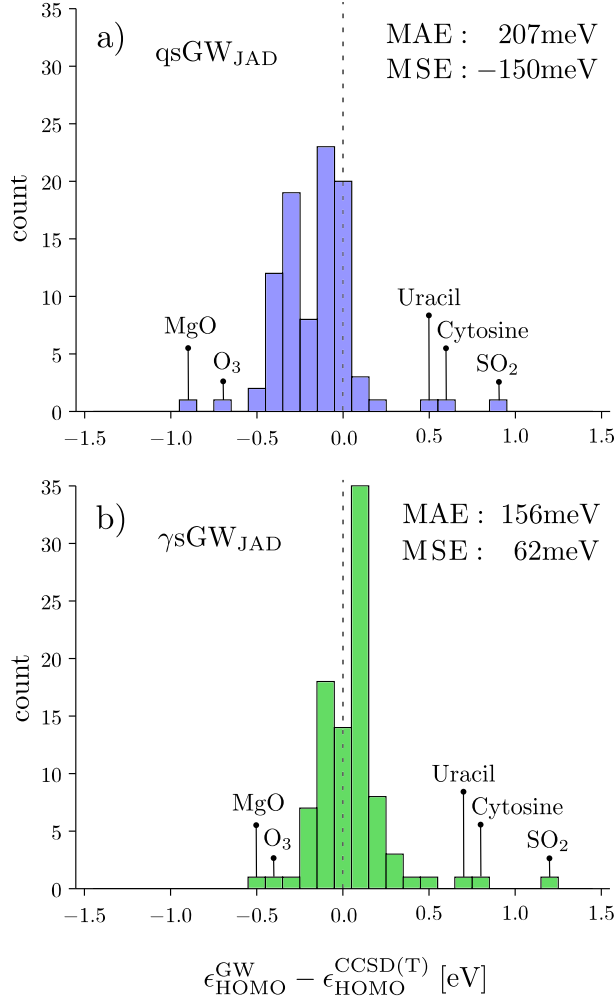


FIG. 4. Histogram of the $(\epsilon_{\text{HOMO}}^{\text{GW}} - \epsilon_{\text{HOMO}}^{\text{CCSD(T)}})$ difference for (a) the qsGW_{JAD} scheme, and (b) the $\gamma\text{sGW}_{\text{JAD}}$ for 93 molecules out of the GW100 test set (see text). Associated mean-absolute-errors (MAE) and mean-signed-errors (MSE) are indicated in each case.

confirmed by Fig. 3 showing in green that the $\gamma\text{sGW}_{\text{JAD}}$ scheme yields results intermediate between that of qsGW and scGW . The outliers remain the same as the one identified within the qsGW and qsGW_{JAD} schemes.

We close our discussion of the JAD process by plotting in Fig. 5 the spectral function $A_n^{\text{GW}}(\omega)$ associated with the carbon-monoxide LUMO at the PBE Kohn-Sham level. We compare the $A_n^{\text{GW}}(\omega)$ obtained with (a) the $\text{evGW@PBE-diag. } \Sigma$ scheme (in grey), (b) the $\text{evGW@PBE-full } \Sigma$ scheme (in red), and (c) the qsGW_{JAD} process (in blue). While the $\text{evGW-diag-}\Sigma$ scheme yields a single quasiparticle peak, but located ~ 0.8 eV away from the qsGW_{JAD} pole, the $\text{evGW-full } \Sigma$ scheme yields several structures, the strongest one ($Z \simeq 0.54$) defining the quasiparticle energy. The

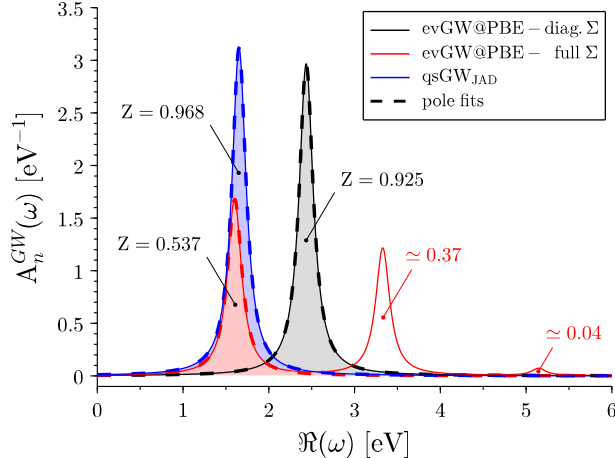


FIG. 5. Plot of the spectral function $A_n^{GW}(\omega)$ associated with the carbon-monoxide LUMO level. We compare the (grey) $evGW@PBE$ -diag. Σ , (red) $evGW@PBE$ -full Σ and (blue) $qsGW_{JAD}$ schemes. Dashed lines are the lorentzian fits of the principal poles with their associated Z spectral weights. An estimation of the spectral weight associated to secondary poles in the $evGW@PBE$ -full Σ case is also provided.

comparison between these two spectral functions indicates that the self-energy operator is strongly non-diagonal in the input PBE Kohn-Sham basis. If we now rotate the input molecular orbitals using the JAD process, the final spectral function becomes dominated by a single quasiparticle peak. Contrary to the $evGW$ -diag. Σ scheme, this is not obtained by enforcing artificially the diagonality of the self-energy operator in the one-body MO basis, but by finding the rotated MOs that maximalize the diagonality of the $G(\epsilon_n^{QP})$ family of matrices, without any approximation on the self-energy operator.

We note that the $evGW$ -full Σ scheme, that does not update the one-body MOs but build G from the full self-energy in the Kohn-Sham basis, yields a main quasiparticle energy in much better agreement with $qsGW_{JAD}$ as compared to the $evGW$ -diag. Σ result. However, the presence of two poles with significant weights may give rise to instabilities, with a dominant spectral weight jumping from one pole to another, with discontinuity of the quasiparticle energy, in a self-consistent process or upon varying a structural parameter (e.g. bond length in the study of a dissociation curve).^{71-73,131}

IV. CONCLUSIONS

We have proposed an alternative approach to quasiparticle self-consistent GW calculations relying on the Joint Approximate Diagonalization (JAD) of the GW Green's function $G(\varepsilon_n^{QP})$ taken at the available ε_n^{QP} quasiparticle energies (input Kohn-Sham energies or previous iteration values in a self-consistent scheme). Such an approach does not rely on the set-up of a symmetrized and static *ansatz* self-energy operator. In the JAD scheme, the approximation lies in the fact that there is no rotated one-body set of molecular orbitals that can strictly diagonalize all $G(\varepsilon_n^{QP})$ matrices, with n ranging from core to unoccupied levels in a very large energy range (a few hundred eVs). Remarkably, even though relying on approximations of seemingly very different nature, this alternative quasiparticle self-consistent scheme provides quasiparticle energies close to the one obtained with the standard qs GW scheme. We cannot exclude potential relations between the principles behind the construction of the effective static symmetrized self-energy of the standard qs GW scheme, and the present approximate diagonalization scheme of the $G(\varepsilon_n^{QP})$ matrices.

We further tested a self-consistent scheme that extends beyond the quasiparticle framework by constructing the density matrix from the GW Green's function through an integral along the imaginary axis, capturing not only the spectral weight of the quasiparticles but also that of the background. Such an approach yields results located in between qs GW and sc GW data, in better agreement with reference CCSD(T) calculations for the set of systems considered. Such a variant can be merged with the standard qs GW scheme but requires calculating the self-energy operator $\Sigma_{XC}^{GW}(i\omega)$ for a set of frequencies along the imaginary axis according to the chosen quadrature.

SUPPLEMENTARY MATERIAL

See the Supplementary Material for a complete Table of the $GW100$ HOMO energies at the various self-consistent levels.

ACKNOWLEDGMENTS

The authors are indebted to insightful discussions with Pierre-François Loos and Antoine Marie. The project received support from the French Agence Nationale de la Recherche (ANR) under contract ANR-20-CE29-0005 (BSE-Forces). Computational resources generously provided by the national HPC facilities under contract GENCI-TGCC A0110910016 are acknowledged.

DATA AVAILABILITY STATEMENT

The data that support the findings of this study are available within the article and its supplementary material.

REFERENCES

- ¹L. Hedin, *Phys. Rev.* **139**, A796 (1965).
- ²D. Golze, M. Dvorak, and P. Rinke, *Front. Chem.* **7**, 377 (2019).
- ³F. Bruneval, N. Dattani, and M. J. van Setten, *Front. Chem.* **9** (2021), [10.3389/fchem.2021.749779](https://doi.org/10.3389/fchem.2021.749779).
- ⁴R. Martin, L. Reining, and D. Ceperley, *Interacting Electrons: Theory and Computational Approaches* (Cambridge University Press, 2016).
- ⁵G. Strinati, H. J. Mattausch, and W. Hanke, *Phys. Rev. Lett.* **45**, 290 (1980).
- ⁶M. S. Hybertsen and S. G. Louie, *Phys. Rev. B* **34**, 5390 (1986).
- ⁷R. W. Godby, M. Schlüter, and L. J. Sham, *Phys. Rev. B* **37**, 10159 (1988).
- ⁸W. von der Linden and P. Horsch, *Phys. Rev. B* **37**, 8351 (1988).
- ⁹M. F. Lange and T. C. Berkelbach, *J. Chem. Theory Comput.* **14**, 4224 (2018), pMID: 30028614, <https://doi.org/10.1021/acs.jctc.8b00455>.
- ¹⁰R. Quintero-Monsebaiz, E. Monino, A. Marie, and P.-F. Loos, *J. Chem. Phys.* **157** (2022), [10.1063/5.0130837](https://doi.org/10.1063/5.0130837), 231102, https://pubs.aip.org/aip/jcp/article-pdf/doi/10.1063/5.0130837/16555472/231102_1_online.pdf.
- ¹¹J. Tölle and G. Kin-Lic Chan, *J. Chem. Phys.* **158** (2023), [10.1063/5.0139716](https://doi.org/10.1063/5.0139716), 124123, https://pubs.aip.org/aip/jcp/article-pdf/doi/10.1063/5.0139716/16794059/124123_1_online.pdf.
- ¹²X. Ren, P. Rinke, V. Blum, J. Wieferink, A. Tkatchenko, A. Sanfilippo, K. Reuter, and M. Scheffler, *New J. Phys.* **14**, 053020 (2012).
- ¹³H. N. Rojas, R. W. Godby, and R. J. Needs, *Phys. Rev. Lett.* **74**, 1827 (1995).
- ¹⁴D. Foerster, P. Koval, and D. Sánchez-Portal, *J. Chem. Phys.* **135** (2011), [10.1063/1.3624731](https://doi.org/10.1063/1.3624731), 074105, https://pubs.aip.org/aip/jcp/article-pdf/doi/10.1063/1.3624731/15440261/074105_1_online.pdf.

- ¹⁵A. Kutepov, K. Haule, S. Y. Savrasov, and G. Kotliar, *Phys. Rev. B* **85**, 155129 (2012).
- ¹⁶J. Wilhelm, D. Golze, L. Talirz, J. Hutter, and C. A. Pignedoli, *J. Phys. Chem. Lett.* **9**, 306 (2018), pMID: 29280376, <https://doi.org/10.1021/acs.jpcclett.7b02740>.
- ¹⁷M. Kim, G. J. Martyna, and S. Ismail-Beigi, *Phys. Rev. B* **101**, 035139 (2020).
- ¹⁸A. Förster and L. Visscher, *J. Chem. Theory Comput.* **16**, 7381 (2020), pMID: 33174743, <https://doi.org/10.1021/acs.jctc.0c00693>.
- ¹⁹I. Duchemin and X. Blase, *J. Chem. Theory Comput.* **17**, 2383 (2021), pMID: 33797245, <https://doi.org/10.1021/acs.jctc.1c00101>.
- ²⁰C. J. Scott, O. J. Backhouse, and G. H. Booth, *J. Chem. Phys.* **158** (2023), 10.1063/5.0143291, 124102, https://pubs.aip.org/aip/jcp/article-pdf/doi/10.1063/5.0143291/16791990/124102_1_online.pdf.
- ²¹D. Neuhauser, Y. Gao, C. Arntsen, C. Karshenas, E. Rabani, and R. Baer, *Phys. Rev. Lett.* **113**, 076402 (2014).
- ²²V. Vlček, E. Rabani, D. Neuhauser, and R. Baer, *J. Chem. Theory Comput.* **13**, 4997 (2017), pMID: 28876912, <https://doi.org/10.1021/acs.jctc.7b00770>.
- ²³T. Stein, H. Eisenberg, L. Kronik, and R. Baer, *Phys. Rev. Lett.* **105**, 266802 (2010).
- ²⁴X. Blase, C. Attaccalite, and V. Olevano, *Phys. Rev. B* **83**, 115103 (2011).
- ²⁵T. Körzdörfer and N. Marom, *Phys. Rev. B* **86**, 041110 (2012).
- ²⁶F. Bruneval and M. A. L. Marques, *J. Chem. Theory Comput.* **9**, 324 (2013), pMID: 26589035, <https://doi.org/10.1021/ct300835h>.
- ²⁷T. Rangel, S. M. Hamed, F. Bruneval, and J. B. Neaton, *J. Chem. Theory Comput.* **12**, 2834 (2016), pMID: 27123935, <https://doi.org/10.1021/acs.jctc.6b00163>.
- ²⁸F. Kaplan, M. E. Harding, C. Seiler, F. Weigend, F. Evers, and M. J. van Setten, *J. Chem. Theory Comput.* **12**, 2528 (2016), pMID: 27168352.
- ²⁹M. P. Surh, J. E. Northrup, and S. G. Louie, *Phys. Rev. B* **38**, 5976 (1988).
- ³⁰M. Rohlfing, P. Krüger, and J. Pollmann, *Phys. Rev. B* **56**, R7065 (1997).
- ³¹M. Shishkin and G. Kresse, *Phys. Rev. B* **75**, 235102 (2007).
- ³²B. Baumeier, D. Andrienko, Y. Ma, and M. Rohlfing, *J. Chem. Theory Comput.* **8**, 997 (2012), pMID: 26593361, <https://doi.org/10.1021/ct2008999>.
- ³³M. R. Filip and F. Giustino, *Phys. Rev. B* **90**, 245145 (2014).
- ³⁴V. Vlček, R. Baer, E. Rabani, and D. Neuhauser, *J. Chem. Phys.* **149**, 174107 (2018).
- ³⁵H. J. de Groot, P. A. Bobbert, and W. van Haeringen, *Phys. Rev. B* **52**, 11000 (1995).

- ³⁶B. Holm and U. von Barth, *Phys. Rev. B* **57**, 2108 (1998).
- ³⁷P. García-González and R. W. Godby, *Phys. Rev. B* **63**, 075112 (2001).
- ³⁸W.-D. Schöne and A. G. Eguiluz, *Phys. Rev. Lett.* **81**, 1662 (1998).
- ³⁹W. Ku and A. G. Eguiluz, *Phys. Rev. Lett.* **89**, 126401 (2002).
- ⁴⁰I.-H. Chu, J. P. Trinastic, Y.-P. Wang, A. G. Eguiluz, A. Kozhevnikov, T. C. Schulthess, and H.-P. Cheng, *Phys. Rev. B* **93**, 125210 (2016).
- ⁴¹M. Grumet, P. Liu, M. Kaltak, J. Klimeš, and G. Kresse, *Phys. Rev. B* **98**, 155143 (2018).
- ⁴²A. L. Kutepov, *Phys. Rev. B* **105**, 045124 (2022).
- ⁴³C.-N. Yeh, S. Iskakov, D. Zgid, and E. Gull, *Phys. Rev. B* **106**, 235104 (2022).
- ⁴⁴K. S. Thygesen and A. Rubio, *Phys. Rev. B* **77**, 115333 (2008).
- ⁴⁵A. Stan, N. E. Dahlen, and R. van Leeuwen, *J. Chem. Phys.* **130** (2009), 10.1063/1.3089567, 114105, https://pubs.aip.org/aip/jcp/article-pdf/doi/10.1063/1.3089567/15424617/114105_1_online.pdf.
- ⁴⁶C. Rostgaard, K. W. Jacobsen, and K. S. Thygesen, *Phys. Rev. B* **81**, 085103 (2010).
- ⁴⁷N. Marom, F. Caruso, X. Ren, O. T. Hofmann, T. Körzdörfer, J. R. Chelikowsky, A. Rubio, M. Scheffler, and P. Rinke, *Phys. Rev. B* **86**, 245127 (2012).
- ⁴⁸F. Caruso, P. Rinke, X. Ren, M. Scheffler, and A. Rubio, *Phys. Rev. B* **86**, 081102 (2012).
- ⁴⁹F. Caruso, P. Rinke, X. Ren, A. Rubio, and M. Scheffler, *Phys. Rev. B* **88**, 075105 (2013).
- ⁵⁰P. Koval, D. Foerster, and D. Sánchez-Portal, *Phys. Rev. B* **89**, 155417 (2014).
- ⁵¹L.-W. Wang, *Phys. Rev. B* **91**, 125135 (2015).
- ⁵²J. W. Knight, X. Wang, L. Gallandi, O. Dolgounitcheva, X. Ren, J. V. Ortiz, P. Rinke, T. Körzdörfer, and N. Marom, *J. Chem. Theory Comput.* **12**, 615 (2016), pMID: 26731609, <https://doi.org/10.1021/acs.jctc.5b00871>.
- ⁵³F. Caruso, M. Dauth, M. J. van Setten, and P. Rinke, *J. Chem. Theory Comput.* **12**, 5076 (2016), pMID: 27631585.
- ⁵⁴L. Hung, F. H. da Jornada, J. Souto-Casares, J. R. Chelikowsky, S. G. Louie, and S. Ögüt, *Phys. Rev. B* **94**, 085125 (2016).
- ⁵⁵M. Wen, V. Abraham, G. Harsha, A. Shee, K. B. Whaley, and D. Zgid, *J. Chem. Theory Comput.* **20**, 3109 (2024), pMID: 38573104, <https://doi.org/10.1021/acs.jctc.3c01279>.
- ⁵⁶G. Harsha, V. Abraham, M. Wen, and D. Zgid, *arXiv:2406.18077* (2024).
- ⁵⁷V. Abraham, G. Harsha, and D. Zgid, *J. Chem. Theory Comput.* **20**, 4579 (2024), pMID: 38778459, <https://doi.org/10.1021/acs.jctc.4c00075>.

- ⁵⁸S. V. Faleev, M. van Schilfgaarde, and T. Kotani, *Phys. Rev. Lett.* **93**, 126406 (2004).
- ⁵⁹M. van Schilfgaarde, T. Kotani, and S. Faleev, *Phys. Rev. Lett.* **96**, 226402 (2006).
- ⁶⁰F. Bruneval, N. Vast, and L. Reining, *Phys. Rev. B* **74**, 045102 (2006).
- ⁶¹S. Ismail-Beigi, *J. Phys.: Cond. Matt.* **29**, 385501 (2017).
- ⁶²A. Svane, N. E. Christensen, I. Gorczyca, M. van Schilfgaarde, A. N. Chantis, and T. Kotani, *Phys. Rev. B* **82**, 115102 (2010).
- ⁶³A. Punya and W. R. L. Lambrecht, *Phys. Rev. B* **85**, 195147 (2012).
- ⁶⁴F. Bruneval and M. Gatti, “Quasiparticle self-consistent gw method for the spectral properties of complex materials,” in *First Principles Approaches to Spectroscopic Properties of Complex Materials*, edited by C. Di Valentin, S. Botti, and M. Cococcioni (Springer Berlin Heidelberg, Berlin, Heidelberg, 2014) pp. 99–135.
- ⁶⁵F. Brivio, K. T. Butler, A. Walsh, and M. van Schilfgaarde, *Phys. Rev. B* **89**, 155204 (2014).
- ⁶⁶J. Lei and T. Zhu, *J. Chem. Phys.* **157**, 214114 (2022), https://pubs.aip.org/aip/jcp/article-pdf/doi/10.1063/5.0125756/16554326/214114_1_online.pdf.
- ⁶⁷S.-H. Ke, *Phys. Rev. B* **84**, 205415 (2011).
- ⁶⁸A. Förster and L. Visscher, *Front. Chem.* **9** (2021), 10.3389/fchem.2021.736591.
- ⁶⁹A. Förster and L. Visscher, *J. Chem. Theory Comput.* **18**, 6779 (2022), pMID: 36201788, <https://doi.org/10.1021/acs.jctc.2c00531>.
- ⁷⁰A. Förster, E. van Lenthe, E. Spadetto, and L. Visscher, *J. Chem. Theory Comput.* **19**, 5958 (2023), pMID: 37594901, <https://doi.org/10.1021/acs.jctc.3c00512>.
- ⁷¹E. Monino and P.-F. Loos, *J. Chem. Phys.* **156**, 231101 (2022), https://pubs.aip.org/aip/jcp/article-pdf/doi/10.1063/5.0089317/16544435/231101_1_online.pdf.
- ⁷²A. Marie and P.-F. Loos, *J. Chem. Theory Comput.* **19**, 3943 (2023), pMID: 37311565, <https://doi.org/10.1021/acs.jctc.3c00281>.
- ⁷³M. VÉril, P. Romaniello, J. A. Berger, and P.-F. Loos, *J. Chem. Theory Comput.* **14**, 5220 (2018), pMID: 30212627, <https://doi.org/10.1021/acs.jctc.8b00745>.
- ⁷⁴M. J. van Setten, F. Caruso, S. Sharifzadeh, X. Ren, M. Scheffler, F. Liu, J. Lischner, L. Lin, J. R. Deslippe, S. G. Louie, C. Yang, F. Weigend, J. B. Neaton, F. Evers, and P. Rinke, *J. Chem. Theory Comput.* **11**, 5665 (2015), pMID: 26642984, <https://doi.org/10.1021/acs.jctc.5b00453>.
- ⁷⁵K. Krause, M. E. Harding, and W. Klopper, *Mol. Phys.* **113**, 1952 (2015), <https://doi.org/10.1080/00268976.2015.1025113>.

- ⁷⁶E. Maggio, P. Liu, M. J. van Setten, and G. Kresse, *J. Chem. Theory Comput.* **13**, 635 (2017), pMID: 28094981, <https://doi.org/10.1021/acs.jctc.6b01150>.
- ⁷⁷M. Govoni and G. Galli, *J. Chem. Theory Comput.* **14**, 1895 (2018), pMID: 29397712, <https://doi.org/10.1021/acs.jctc.7b00952>.
- ⁷⁸W. Gao and J. R. Chelikowsky, *J. Chem. Theory Comput.* **15**, 5299 (2019), pMID: 31424933, <https://doi.org/10.1021/acs.jctc.9b00520>.
- ⁷⁹A. Förster and L. Visscher, *J. Chem. Theory Comput.* **17**, 5080 (2021), pMID: 34236172, <https://doi.org/10.1021/acs.jctc.1c00308>.
- ⁸⁰J.-F. Cardoso and A. Souloumiac, *SIAM J. Matrix Anal. Appl.* **17**, 161 (1996), <https://doi.org/10.1137/S0895479893259546>.
- ⁸¹F. Aryasetiawan and O. Gunnarsson, *Rep. Prog. Phys.* **61**, 237 (1998).
- ⁸²B. Farid, *Electron Correlation in the Solid State - Chapter 3*, edited by N. March (Imperial College Press, London, 1999).
- ⁸³G. Onida, L. Reining, and A. Rubio, *Rev. Mod. Phys.* **74**, 601 (2002).
- ⁸⁴Y. Ping, D. Rocca, and G. Galli, *Chem. Soc. Rev.* **42**, 2437 (2013).
- ⁸⁵O. J. Backhouse and G. H. Booth, *J. Chem. Theory Comput.* **16**, 6294 (2020), pMID: 32886508, <https://doi.org/10.1021/acs.jctc.0c00701>.
- ⁸⁶S. J. Bintrim and T. C. Berkelbach, *J. Chem. Phys.* **154**, 041101 (2021), https://pubs.aip.org/aip/jcp/article-pdf/doi/10.1063/5.0035141/13941773/041101_1_online.pdf.
- ⁸⁷J. McClain, J. Lischner, T. Watson, D. A. Matthews, E. Ronca, S. G. Louie, T. C. Berkelbach, and G. K.-L. Chan, *Phys. Rev. B* **93**, 235139 (2016).
- ⁸⁸E. Monino and P.-F. Loos, *J. Chem. Phys.* **159**, 034105 (2023), https://pubs.aip.org/aip/jcp/article-pdf/doi/10.1063/5.0159853/18045407/034105_1_5.0159853.pdf.
- ⁸⁹X. Blase, C. Attaccalite, and V. Olevano, *Phys. Rev. B* **83**, 115103 (2011).
- ⁹⁰I. Duchemin and X. Blase, *J. Chem. Theory Comput.* **16**, 1742 (2020), pMID: 32023052, <https://doi.org/10.1021/acs.jctc.9b01235>.
- ⁹¹J. P. Perdew, M. Ernzerhof, and K. Burke, *J. Chem. Phys.* **105**, 9982 (1996), https://pubs.aip.org/aip/jcp/article-pdf/105/22/9982/9439202/9982_1_online.pdf.
- ⁹²J. P. Perdew, K. Burke, and M. Ernzerhof, *Phys. Rev. Lett.* **77**, 3865 (1996).
- ⁹³J. Dunning, Thom H., *J. Chem. Phys.* **90**, 1007 (1989), https://pubs.aip.org/aip/jcp/article-pdf/90/2/1007/18974738/1007_1_online.pdf.

- ⁹⁴R. A. Kendall, J. Dunning, Thom H., and R. J. Harrison, *J. Chem. Phys.* **96**, 6796 (1992), https://pubs.aip.org/aip/jcp/article-pdf/96/9/6796/18998924/6796_1_online.pdf.
- ⁹⁵R. Sarkar, M. Boggio-Pasqua, P.-F. Loos, and D. Jacquemin, *J. Chem. Theory Comput.* **17**, 1117 (2021), pMID: 33492950, <https://doi.org/10.1021/acs.jctc.0c01228>.
- ⁹⁶J. Villalobos-Castro, I. Knysh, D. Jacquemin, I. Duchemin, and X. Blase, *J. Chem. Phys.* **159**, 024116 (2023), https://pubs.aip.org/aip/jcp/article-pdf/doi/10.1063/5.0156687/18037481/024116_1_5.0156687.pdf.
- ⁹⁷C. A. McKeon, S. M. Hamed, F. Bruneval, and J. B. Neaton, *J. Chem. Phys.* **157**, 074103 (2022), https://pubs.aip.org/aip/jcp/article-pdf/doi/10.1063/5.0097582/16547598/074103_1_online.pdf.
- ⁹⁸A. R. Kshirsagar and R. Poloni, *J. Phys. Chem. A* **127**, 2618 (2023), pMID: 36913525, <https://doi.org/10.1021/acs.jpca.2c07526>.
- ⁹⁹A. R. Kshirsagar, G. D'Avino, X. Blase, J. Li, and R. Poloni, *J. Chem. Theory Comput.* **16**, 2021 (2020), pMID: 32097003, <https://doi.org/10.1021/acs.jctc.9b01257>.
- ¹⁰⁰Y. Jin, N. Q. Su, and W. Yang, *J. Phys. Chem. Lett.* **10**, 447 (2019), <https://doi.org/10.1021/acs.jpcelett.8b03337>.
- ¹⁰¹J. Li and W. Yang, *J. Phys. Chem. Lett.* **13**, 9372 (2022), pMID: 36190273, <https://doi.org/10.1021/acs.jpcelett.2c02051>.
- ¹⁰²J. Li, Y. Jin, P. Rinke, W. Yang, and D. Golze, *J. Chem. Theory Comput.* **18**, 7570 (2022), pMID: 36322136, <https://doi.org/10.1021/acs.jctc.2c00617>.
- ¹⁰³X. Ren, N. Marom, F. Caruso, M. Scheffler, and P. Rinke, *Phys. Rev. B* **92**, 081104 (2015).
- ¹⁰⁴R. Del Sole, L. Reining, and R. W. Godby, *Phys. Rev. B* **49**, 8024 (1994).
- ¹⁰⁵A. Schindlmayr and R. W. Godby, *Phys. Rev. Lett.* **80**, 1702 (1998).
- ¹⁰⁶F. Bruneval and A. Förster, *J. Chem. Theory Comput.* **20**, 3218 (2024), pMID: 38603811, <https://doi.org/10.1021/acs.jctc.4c00090>.
- ¹⁰⁷M. Shishkin, M. Marsman, and G. Kresse, *Phys. Rev. Lett.* **99**, 246403 (2007).
- ¹⁰⁸P. Romaniello, S. Guyot, and L. Reining, *J. Chem. Phys.* **131**, 154111 (2009), https://pubs.aip.org/aip/jcp/article-pdf/doi/10.1063/1.3249965/13493813/154111_1_online.pdf.
- ¹⁰⁹G. Stefanucci, Y. Pavlyukh, A.-M. Uimonen, and R. van Leeuwen, *Phys. Rev. B* **90**, 115134 (2014).

- ¹¹⁰E. Maggio and G. Kresse, *J. Chem. Theory Comput.* **13**, 4765 (2017), pMID: 28873298, <https://doi.org/10.1021/acs.jctc.7b00586>.
- ¹¹¹A. M. Lewis and T. C. Berkelbach, *J. Chem. Theory Comput.* **15**, 2925 (2019), pMID: 30933508, <https://doi.org/10.1021/acs.jctc.8b00995>.
- ¹¹²V. Vlček, *J. Chem. Theory Comput.* **15**, 6254 (2019), pMID: 31557012, <https://doi.org/10.1021/acs.jctc.9b00317>.
- ¹¹³A. L. Kutepov, *J. Phys.: Cond. Mat.* **33**, 485601 (2021).
- ¹¹⁴A. Förster and L. Visscher, *Phys. Rev. B* **105**, 125121 (2022).
- ¹¹⁵C. H. Patterson, *J. Chem. Theory Comput.* **20**, 7479 (2024), pMID: 39189378, <https://doi.org/10.1021/acs.jctc.4c00795>.
- ¹¹⁶S. Vacondio, D. Varsano, A. Ruini, and A. Ferretti, *J. Chem. Theory Comput.* **20**, 4718 (2024), pMID: 38772396, <https://doi.org/10.1021/acs.jctc.4c00100>.
- ¹¹⁷D. Zhang, N. Q. Su, and W. Yang, *J. Phys. Chem. Lett.* **8**, 3223 (2017), pMID: 28654275, <https://doi.org/10.1021/acs.jpcclett.7b01275>.
- ¹¹⁸R. Orlando, P. Romaniello, and P.-F. Loos, *J. Chem. Phys.* **159**, 184113 (2023), https://pubs.aip.org/aip/jcp/article-pdf/doi/10.1063/5.0176898/18208588/184113_1_5.0176898.pdf.
- ¹¹⁹J. L. Whitten, *J. Chem. Phys.* **58**, 4496 (1973), https://pubs.aip.org/aip/jcp/article-pdf/58/10/4496/18884936/4496_1_online.pdf.
- ¹²⁰O. Vahtras, J. Almlöf, and M. Feyereisen, *Chem. Phys. Lett.* **213**, 514 (1993).
- ¹²¹I. Duchemin, J. Li, and X. Blase, *J. Chem. Theory Comput.* **13**, 1199 (2017), pMID: 28094983, <https://doi.org/10.1021/acs.jctc.6b01215>.
- ¹²²M. Kehry, W. Klopper, and C. Holzer, *J. Chem. Phys.* **159**, 044116 (2023), https://pubs.aip.org/aip/jcp/article-pdf/doi/10.1063/5.0160265/18064976/044116_1_5.0160265.pdf.
- ¹²³R. L. Panadés-Barrueta and D. Golze, *J. Chem. Theory Comput.* **19**, 5450 (2023), pMID: 37566917, <https://doi.org/10.1021/acs.jctc.3c00555>.
- ¹²⁴F. Weigend and R. Ahlrichs, *Phys. Chem. Chem. Phys.* **7**, 3297 (2005).
- ¹²⁵F. Weigend, M. Häser, H. Patzelt, and R. Ahlrichs, *Chem. Phys. Lett.* **294**, 143 (1998).
- ¹²⁶F. Neese, F. Wennmohs, U. Becker, and C. Riplinger, *J. Chem. Phys.* **152**, 224108 (2020), https://pubs.aip.org/aip/jcp/article-pdf/doi/10.1063/5.0004608/16740678/224108_1_online.pdf.

- ¹²⁷C. Adamo and V. Barone, *J. Chem. Phys.* **110**, 6158 (1999), https://pubs.aip.org/aip/jcp/article-pdf/110/13/6158/19068890/6158_1_online.pdf.
- ¹²⁸The HOMO energy for the C_8H_8 cyclooctatetraene amounts in Ref. 53 to -9.30 eV and -7.81 eV at the *qsGW* and *scGW* level, respectively. This yields an unusually large error for the *qsGW* scheme as compared to the -8.35 eV CCSD(T) result and to our *qsGW*-JAD value of -8.42 eV.
- ¹²⁹Such values are also close to the SRG-*qsGW* deviation with respect to CCSD(T) as obtained in Ref. 72 for the aug-cc-pVTZ HOMO energies of the *GW50* subset, with a MSE/MAE of -0.17 eV/0.19 eV, respectively.
- ¹³⁰This deviation for the *scGW* scheme as compared to CCSD(T) is consistent with the 0.20 eV/0.24 eV MSE/MAE values obtained in Ref. 56 on a different 29 molecules subset and at the cc-pVQZ level.
- ¹³¹J. A. Berger, P.-F. Loos, and P. Romaniello, *J. Chem. Theory Comput.* **17**, 191 (2021), pMID: 33306908, <https://doi.org/10.1021/acs.jctc.0c00896>.